

Elastic and Inelastic Proton Scattering on Si<sup>29</sup>

C. P. Poirier, J. Walinga,\* J. C. Manthuruthil, and Gale I. Harris

Aerospace Research Laboratories,† Wright-Patterson Air Force Base, Ohio 45433

(Received 28 January 1970)

High-resolution measurements of the differential cross section for elastic proton scattering on Si<sup>29</sup> have been performed in the energy range  $E_p = 1.1$ – $2.5$  MeV, which corresponds to the range  $E_x(\text{P}^{30}) = 6.7$ – $8.1$  MeV. Twenty-four resonances were observed, including ten previously unreported resonances. For all but two resonances, the proton orbital momenta were determined, and, in many cases, unique spin assignments were made. Partial proton widths or strengths are given for all resonances. Five  $1^-$  resonances were observed with the unusually large total  $p$ -wave reduced width  $\theta_p^2 = 1.14$  in the elastic channel. Similarly, four  $2^-$  resonances appear with a total  $p$ -wave reduced width  $\theta_p^2 = 0.68$ . For the  $1^-$  resonances, both  $p_{1/2}$  and  $p_{3/2}$  elastic scattering contribute strongly. Two definite, and one probable,  $4^-$  resonances were observed with a total  $f$ -wave reduced width  $\theta_p^2 = 0.15$ . The yield of inelastically scattered protons from the first excited state of Si<sup>29</sup> was measured in the energy range  $E_p = 1.9$ – $2.5$  MeV. Eleven resonances were observed, including three previously unreported resonances. The resonance strengths were measured relative to the known strength of the 1302-keV resonance in the Si<sup>29</sup>( $p, \gamma$ )P<sup>30</sup> reaction. For the resonances with known spin, the partial inelastic proton widths were obtained.

## I. INTRODUCTION

A recent investigation of the properties of the energy levels of P<sup>30</sup> has been performed by means of the Si<sup>29</sup>( $p, \gamma$ )P<sup>30</sup> reaction.<sup>1</sup> This work provided extensive data on the bound states below  $E_x = 5$  MeV, and on the resonance levels in the region  $5.9 \leq E_x \leq 7.4$  MeV corresponding to proton bombarding energies  $0.3 \leq E_p \leq 1.8$  MeV. An interesting result was the observation in the resonance region of several odd-parity levels ( $J = 1, 2,$  and  $4$ ) with unusually large proton reduced widths ( $\sim 20\%$  of the Wigner limit). A few of these levels could be identified as  $T = 1$  analog states, although clear evidence of significant isospin mixing appears in at least two cases. The  $\gamma$ -ray decay properties of several other levels of this type show they must be fairly pure  $T = 0$  states. Although significant configuration and isospin mixing is revealed by the data, it is clear that the observed odd-parity spectrum is relatively simple in comparison with the even-parity spectra in this mass region.

The particular interest in the odd-parity resonance states coupled with the fact that information available from other reactions is incomplete motivated the present investigation of elastic and inelastic proton scattering on Si<sup>29</sup> in the energy region  $1.1 \leq E_p \leq 2.5$  MeV. Elastic scattering is especially helpful in the study of properties of most of the resonance states and, in particular, the broad odd-parity levels. When combined with the results of ( $p, \gamma$ ) work, it can lead to unique spin-parity assignments, partial proton widths, and reduced proton widths for the resonance levels.

The Si<sup>29</sup>( $p, p$ )Si<sup>29</sup> reaction has been studied previously by Storizhko and Popov,<sup>2</sup> and L'vov *et al.*<sup>3</sup> In the energy region  $1.1 \leq E_p \leq 2.5$  MeV, they observed 15 resonances; however, one of these ( $E_p = 2083$  keV) must be attributed to the Si<sup>28</sup>( $p, p$ )Si<sup>28</sup> reaction (see Sec. IV). Detailed analysis was performed for only eight resonances, yielding six spin assignments and natural widths ranging from 4 to 24 keV. The same group<sup>3</sup> carried out inelastic scattering measurements in which eight resonances were observed in the energy region considered. No details except resonance energies, total widths, and unanalyzed angular-distribution data were reported.

In the energy region under consideration, the only open channels for proton induced reactions are ( $p, \gamma$ ), ( $p, p'\gamma$ ), and ( $p, p$ ). It is clear that a knowledge of the inelastic proton strengths is important in the analysis of the elastic scattering data. This paper reports the results of high-resolution measurements and the analysis of elastic and inelastic proton scattering on Si<sup>29</sup> with a simultaneous measurement of the ( $p, \gamma$ ) yield in the energy range  $1.1 \leq E_p \leq 2.5$  MeV. A total of 29 ( $p, \gamma$ ) resonances in this energy range have been reported. These include the 18 resonances between  $E_p = 1.1$  and  $1.8$  MeV studied by Harris, Hyder, and Walinga,<sup>1</sup> nine resonances between  $1.4$  and  $1.9$  MeV studied by Bergström-Rohlin,<sup>4</sup> 12 resonances between  $1.4$  and  $2.2$  MeV reported by Phelps, Milne, and Handler,<sup>5</sup> and 20 resonances between  $1.2$  and  $2.5$  MeV reported by L'vov *et al.*<sup>3</sup> For other work on P<sup>30</sup>, the reader is referred to the survey article by Endt and van der Leun.<sup>6</sup>

A measurable elastic scattering contribution appears at 18 of the 29 known ( $p, \gamma$ ) resonances, and inelastic scattering was observed at six of these resonances. Four resonances have been observed to emit only elastic and inelastic protons, and two appear only as elastic scattering resonances. A survey of all known resonances in the energy region under consideration is given in Table I.

An interesting example of the resolution obtained in the present work can be found in the 1506-keV doublet, which was previously unre-

solved. The doublet members are separated by only  $0.7 \pm 0.1$  keV and have natural widths of  $15 \pm 2$  and  $22 \pm 2$  eV, respectively. For details, see Sec. IV.

The strong odd-parity states which characterize this energy region are the subject of model calculations now in progress.<sup>7,8</sup> In this paper, we refrain from making detailed comparisons of results with these preliminary model calculations.

The experimental procedures are given in Sec. II. Section III deals with the method of analysis. Section IV contains the results of both the elastic

TABLE I. Resonances in the Si<sup>29</sup>+ $p$  reactions.

	$(p, \gamma)$ (keV)		$(p, p' \gamma)$ (keV)		$(p, p)$ (keV)		
	Harris <i>et al.</i> <sup>a</sup>	Phelps <i>et al.</i> <sup>b</sup>	L'vov <i>et al.</i> <sup>c</sup>	L'vov <i>et al.</i> <sup>c</sup>	This work	L'vov <i>et al.</i> <sup>c</sup>	This work
1111							
1302			1306				1302
1324							
1327			1331			1331	1327
1374			1377			1377	1373
1470	1470		1470			1470	1472
1502							1502
1505 <sup>d</sup>	1506		1506				1506 <sup>d</sup>
1643	1637		1648			1648	1641
1664							1667
1669	1667						1672
1686	1688	1686				1686	1686
1746		1749					
1749	1752	1753					
1773							
1775	1775	1773					
1792	(1803)					1804	1790
1860							
1975		1967	1967	1969		1967	1969
2033		2039	2039	2040			2040
	2075	2081				2063	2059
	2117	2115	2081	2084		2081	2084
		2125					2125
				2229			2229
		2235	2235	2234		2238	2229
		2242				2235	2234
		2308	2308	2314			
				2337			2337
				2351			
				2367			2367
		2371					
			2393 <sup>e</sup>			2393 <sup>e</sup>	
		2407	2407	2412		2412	2412
				2418			2418
							2492
			2491	2495		2491	2495

<sup>a</sup>See Ref. 1.

<sup>b</sup>See Ref. 5.

<sup>c</sup>See Ref. 3.

<sup>d</sup>The 1505-keV resonance was observed as a doublet in the ( $p, p$ ) reaction and confirmed in the ( $p, \gamma$ ) work of Ref. 1.

<sup>e</sup>The 2393-keV resonance of Ref. 3 appeared as a broad effect in our inelastic yield data, but the elastic data could not be fit with a single resonance effect. See text for details.

and inelastic reactions, and Sec. V contains a summary and discussion of the results.

## II. EXPERIMENTAL PROCEDURE

The experiments were performed with the proton beam from the Aerospace Research Laboratories (ARL) 8-MeV insulating core transformer (ICT) tandem accelerator. The measurements were performed with 0.5–1.0- $\mu$ A beam currents, collimated and focused to an approximately 2-mm-diam spot size at the target. The energy resolution of the beam was approximately 200 eV.

The targets were prepared by evaporating SiO<sub>2</sub> enriched<sup>9</sup> in Si<sup>29</sup> onto 10- $\mu$ g/cm<sup>2</sup>-thick carbon foils for the elastic scattering measurements and onto 10-mil-thick silver blanks soldered onto brass cooling disks for the inelastic scattering measurements. Target thicknesses were typically 0.5–1.0 keV and 2.0–3.0 keV at  $E_p = 2.3$  MeV for the elastic and inelastic runs, respectively. The evaporations were done with an electron gun and a carbon crucible in order to avoid contaminants such as Ta and Fe on the elastic scattering targets.

The elastic scattering measurements were made in an ORTEC, 17-in. scattering chamber with four surface barrier detectors placed at angles of 90, 130, 140 and 150° with respect to the beam direction and at a distance of 10 cm from the target. The detectors have a 50-mm<sup>2</sup> sensitive area and 25-keV resolution. Simultaneous ( $p, \gamma$ ) measurements were made with a 1 $\frac{1}{4}$ -in.-diam by 2-in.-long NaI(Tl) detector inside the scattering chamber at a distance of about 0.5 in. from the target. The particle spectra were recorded in four 1024-channel subsections of a 4096-channel analyzer via a routing system. An on-line PDP-8 computer was used to extract from the spectra at each energy point the counts due to elastic scattering from Si<sup>29</sup>. The computer is programmed to locate automatically the Si<sup>29</sup> peak in each of the four subsections of the analyzer memory and to print out the sum of the channel contents over the peak. This method has several advantages over the usual method of using single-channel analyzers for each angle, the most important of which is that it corrects automatically for energy shifts in the particle spectra.

The yield of inelastically scattered protons from Si<sup>29</sup> was obtained by measuring the yield of the 1.273-MeV  $\gamma$  ray from the first excited state of Si<sup>29</sup>. A 5-in.-diam by 5-in.-long NaI(Tl) detector placed at an angle of 55° with respect to the beam direction, and at a distance of 4 in. from the target, was used to detect the 1.273-MeV  $\gamma$  ray. The relative intensities of the inelastic re-

sonances were determined by measuring the areas under the yield curve. In order to obtain the resonance strengths

$$S_{pp'} = (2J+1)\Gamma_p \Gamma_{p'}/\Gamma_t,$$

reported here, the relative strengths of the ( $p, \gamma$ ) and ( $p, p'\gamma$ ) reaction channels of the  $E_p = 1969$ -keV resonance were measured. The absolute  $\gamma$ -ray strength,

$$S_{p\gamma} = (2J+1)\Gamma_p \Gamma_\gamma/\Gamma_t,$$

of the 1969-keV resonance was then determined by comparing its strength with that of the 1302-keV resonance previously measured by Harris, Hyder, and Walinga.<sup>1</sup> This relative strength measurement thus links all the inelastic resonance strengths to a known ( $p, \gamma$ ) resonance strength.

The elastic and inelastic measurements were made in the energy regions  $E_p = 1.1$ –2.5, and 1.9–2.5 MeV, respectively, with energy steps varying from several keV down to 130 eV depending on the local structure of the resonance yield. The proton energy was calibrated by use of the  $E_p = 991.90 \pm 0.04$ -keV resonance in the Al<sup>27</sup>( $p, \gamma$ )Si<sup>28</sup> reaction as the reference point. Standard relativistic corrections were applied.

## III. ANALYSIS

The ground-state spin of Si<sup>29</sup> is  $\frac{1}{2}$  so that both channel spins  $s = 0$  and 1 are possible. Orbital mixing is possible only with  $s = 1$  so that resonance formation can occur with either a unique  $l$  value for the incoming proton and a mixture of channel spins, or with a unique channel spin and a mixture of proton orbital momenta. In the special case of  $J^\pi = 1^-$  resonances, the channel-spin intensity mixing, defined by

$$\zeta = \frac{\text{formation with } s = 1}{\text{total formation}},$$

is equal to the population parameter  $P(1) = 1 - P(0)$ . In those cases where this parameter is known from ( $p, \gamma$ ) work,<sup>1</sup> its value was used in analysis. The parameter  $\zeta$  is related to the channel-spin mixing ratio  $t$  used in Ref. 1 by  $\zeta = t/(1+t)$ . The orbital-mixing amplitude, defined by

$$\epsilon = \frac{\text{formation with } l+2}{\text{formation with } l},$$

has no simple relation to the  $P(m)$  so that its value must be deduced from the fit. Only  $l$  values up to  $g$ -wave scattering and values  $J \leq 4$  were considered in the analysis. Higher values can be ruled out on the basis of Wigner-limit considerations.

In general, the analysis of the elastic scattering data followed the same methods described in a previous paper by one of the authors.<sup>10</sup> Briefly, the experimental data are corrected for a possible background from other isotopes and then compared to the theoretical differential cross section given by the formalism of Blatt and Biedenharn.<sup>11</sup> An instrumental resolution function which takes into account both machine resolution and target spread was folded into the theoretical expressions. The resolution function for each target was obtained by examining the experimental shapes of those  $(p, \gamma)$  resonances which have a total width  $\ll$  the target thickness. As a good approximation to the resolution function, a nonsymmetric triangle with a full width at half maximum approximately equal to the total energy spread was used in the analysis. The comparison between theory and experiment was made after normalizing both to the Rutherford scattering contribution.

A set of computer programs was used to minimize the goodness-of-fit parameter  $\chi^2$  with respect to the resonance energy  $E_0$ , the partial proton width  $\Gamma_p$ , and the total width  $\Gamma_t$  for a given set of the remaining resonance parameters  $l, J, \zeta$ , and  $\epsilon$ . The programs accept as input data the measured values of the yield over the resonance region at each angle. For all the results present-

ed in this paper, the acceptability of any solution was based on a consideration of the 0.1% confidence limit for the goodness-of-fit parameter  $\chi^2$  for each particular set of data.

In many cases, more than one resonance contributed to the measured yield and in such cases interference effects must be considered. The extension of the methods outlined above to the case of two or more interfering resonances is based on the formalism of Blatt and Biedenharn.<sup>11</sup> (A detailed description of the interference effects for even-even nuclei is presented in Ref. 12.) The extension to odd- $A$  nuclei is quite similar to that presented in Ref. 12 except for the addition of channel-spin and orbital-momentum mixing.

#### IV. RESULTS

##### A. Inelastic Proton Scattering

The yield of the 1.273-MeV  $\gamma$  ray from the  $\text{Si}^{29}(p, p'\gamma)\text{Si}^{29}$  reaction is shown in Fig. 1. Eleven resonances were observed, including three previously unobserved resonances at  $E_p = 2229, 2334,$  and  $2351$  keV. The resonance energies and absolute strengths  $S_{pp'}$  are given in Table II. In general, there is good agreement between our results and the previous measurements of L'vov

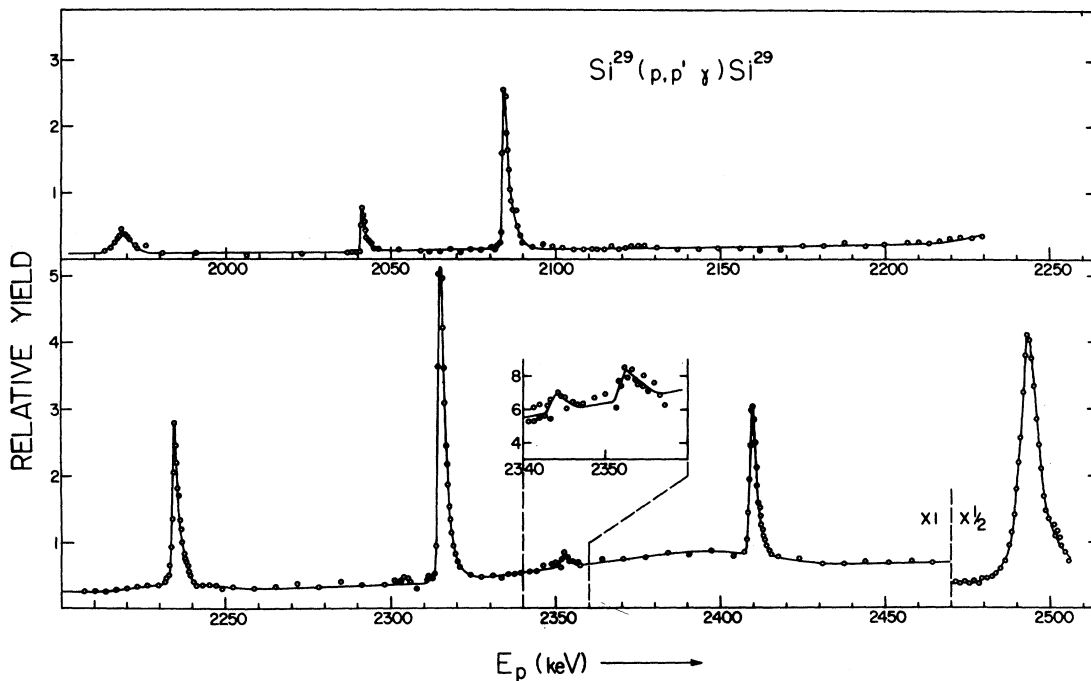


FIG. 1. Yield curve of the 1.273-MeV  $\gamma$  ray from the  $\text{Si}^{29}(p, p'\gamma)\text{Si}^{29}$  reaction in the energy range  $E_p = 1950$ – $2510$  KeV, measured with a 5-in. NaI(Tl) detector at  $55^\circ$  relative to the beam direction. The yield was measured using a 2-keV-thick target. The apparent discrepancy between the energy scale of the inert and the resonance energies reported in the tables is due to carbon buildup on the target.

TABLE II. Inelastic resonance energies and strengths.

$E_p$ (keV)	$(2J+1)\Gamma_p\Gamma_p/\Gamma_t$ (eV)
1968.6 ± 0.5	32 ± 7
2039.8 ± 0.5	19 ± 4
2083.8 ± 0.5	100 ± 20
2228.7 ± 1.0	43 ± 9
2234.1 ± 0.5	110 ± 20
2314.2 ± 0.5	240 ± 50
2337.0 ± 1.0	4 ± 2
2351.0 ± 1.0	7 ± 2
2393 <sup>a</sup>	380 ± 80
2410.6 ± 0.5	120 ± 30
2494.9 ± 1.0	1300 ± 300

<sup>a</sup>Broad peak corresponding to resonances at  $E_p = 2367$  and 2418 keV in the  $(p, p)$  data.

*et al.*<sup>3</sup> in so far as a comparison can be made.

In the analysis of the elastic scattering data, the strengths listed in Table II were used to obtain the partial proton width  $\Gamma_p$  and total natural width  $\Gamma_t$  for each of the resonances in question, since all other decay channels are closed in this energy region.

#### B. Elastic Proton Scattering

The yield of protons elastically scattered from  $\text{Si}^{29}$ , observed at four angles as a function of proton energy, is shown in Figs. 2–15. The proton yields are plotted in units of the Rutherford contribution after background subtraction. The smooth curves are the results of the analysis, as discussed in Sec. III. For most of the resonances, the  $(p, \gamma)$  yield is also given. The apparent discrepancy between the resonance energy in the  $(p, p)$  and  $(p, \gamma)$  channels for some of the resonances is due to carbon build-up on the target.

In the energy region  $E_p < 1.8$  MeV, an intensive search was made at the known locations of the  $(p, \gamma)$  resonances.<sup>1</sup> For the  $(p, \gamma)$  resonances at  $E_p = 1111, 1324, 1746, 1749, 1773$ , and 1775 keV no measurable elastic yield was found. An upper limit of  $S_{pp} \leq 40$  eV can be given for these resonances. At the energies of the other  $(p, \gamma)$  resonances, a clear  $(p, p)$  resonance yield was found.

The 1302-keV resonance is known to have  $J = 1$  from previous  $(p, \gamma)$  work.<sup>1</sup> The solid curve in Fig. 2 shows the  $l = 0, J^\pi = 1^+$  fit to the 1302-keV elastic data. The over-all  $\chi^2 = 0.26$  with a 0.1% confidence limit of  $\chi^2 = 1.72$ . However, the  $l = 1, J^\pi = 1^-$  fit (shown as the dashed curve in Fig. 2) cannot be excluded on the basis of the 0.1% confidence limit since the over-all  $\chi^2$  for this assignment is 0.43. Nevertheless, the data qualitatively favor the  $l = 0$  assignment.

A weak  $(p, \gamma)$  resonance at 1502 keV was repor-

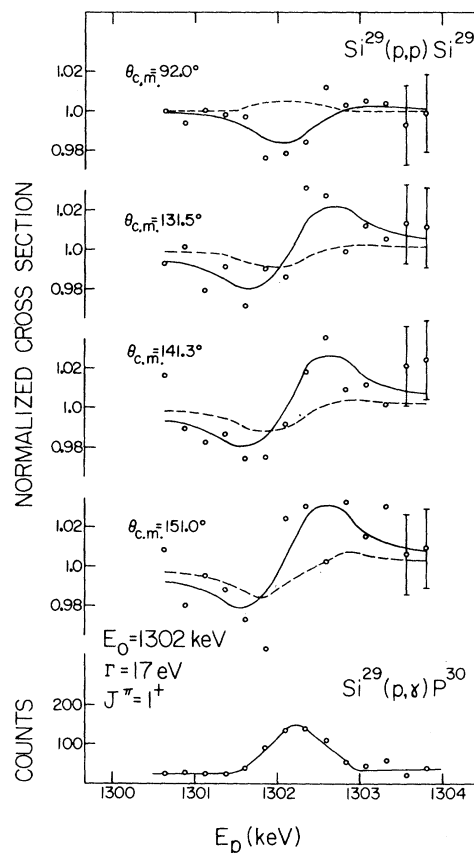


FIG. 2. The differential cross section at four angles for elastic proton scattering on  $\text{Si}^{29}$  in units of the Rutherford contribution at the  $E_p = 1302$ -keV resonance. The solid curve is the theoretical fit for  $J^\pi = 1^+$ . The lower curve shows the simultaneous  $(p, \gamma)$  yield.

ted in Refs. 1 and 4, and is also observed in the present  $(p, p)$  work. The data are shown in the left-hand portion of Fig. 6. No information concerning  $l$  or  $J$  values for this resonance could be extracted from the data. Only a strength  $S_{pp}$  could be determined. However, some recent work<sup>13</sup> in this laboratory on this resonance indicates that an  $l = 3$  assignment is required.

The thin target ( $\sim 500$  eV thick) elastic yield over the 1506-keV resonance region is shown in the right-hand proton of Fig. 6. (See also Fig. 27 in Ref. 1.) The data clearly show a doublet structure with a separation energy of  $700 \pm 100$  eV. The analysis of these data resulted in an  $l = 3, J^\pi = 2^-$  or  $4^-$  assignment for both members of the doublet in agreement with the  $4^-$  assignment for the 1506-keV resonance from  $(p, \gamma)$  work. A careful measurement of the  $\gamma$ -ray spectra at both resonances showed no significant difference in their decays, indicating a  $J^\pi = 4^-$  assignment for both members of the doublet.<sup>1</sup>

Because of the large width of the 1641-keV re-

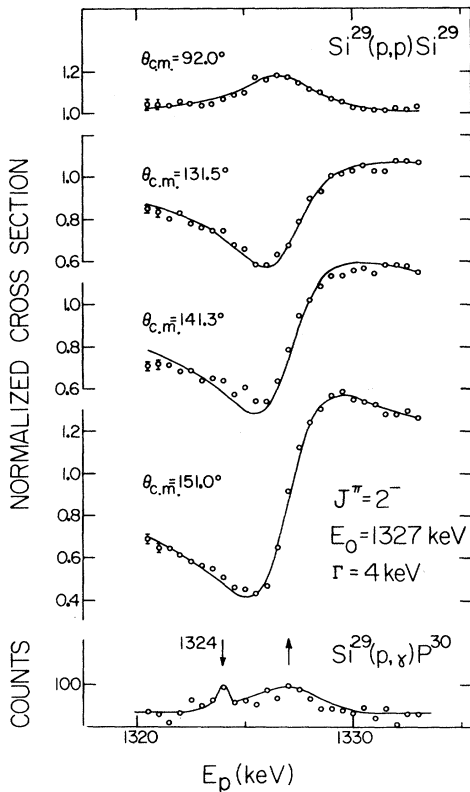


FIG. 3. The differential cross section at four angles for elastic proton scattering on  $\text{Si}^{29}$  in units of the Rutherford contribution at the  $E_p = 1327$ -keV resonance. The smooth curve is the theoretical fit for the indicated  $J^\pi$  and  $\Gamma$ . The lower curve shows the  $(p, \gamma)$  yield.

sonance, interference effects between the 1641-, 1667-, 1672-, and 1686-keV resonances were considered in the analysis. The data for the 1667- and 1672-keV resonances are shown in Fig. 7. The data for the 1641- and 1686-keV resonances are shown in Fig. 8. We attribute the poor fit to the 1686-keV data to a large contribution of sum pulses in the  $\text{Si}^{29}$  channel due to the strong  $\text{C}^{12}(p, p)\text{C}^{12}$  resonances at  $E_p = 1698$  and  $1748$  keV. Attempts to correct for the carbon background were unsuccessful. However, qualitatively the  $J^\pi = 2^-$  assignment from the  $(p, \gamma)$  work is consistent with the elastic scattering data. A similar difficulty was encountered in the elastic scattering work on  $\text{Mg}^{26}$ .<sup>12</sup>

Above 1.8 MeV, new  $(p, p)$  resonances were observed at  $E_p = 2040, 2125, 2337,$  and  $2492$  keV. The 2040- and 2125-keV resonances were observed in previous  $(p, \gamma)$  work.<sup>3,5</sup> To the extent that comparisons can be made, there is agreement between the results reported here and previous elastic scattering work with one exception—the resonance at  $E_p = 2089$  keV. This resonance

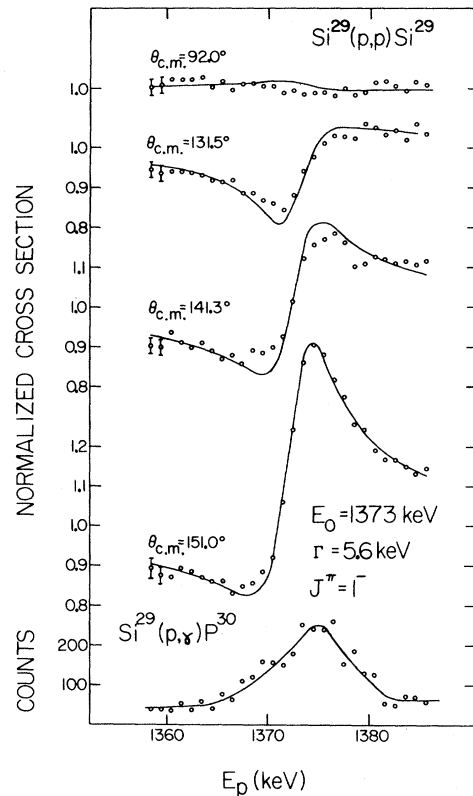


FIG. 4. The differential cross section at four angles for elastic proton scattering on  $\text{Si}^{29}$  in units of the Rutherford contribution at the  $E_p = 1373$ -keV resonance. The smooth curve is the theoretical fit for the indicated  $J^\pi$  and  $\Gamma$ . The lower curve shows the  $(p, \gamma)$  yield.

was observed in the present experiment; however, the amplitude of yields measured with targets of varying relative enrichments of  $\text{Si}^{28}$  and  $\text{Si}^{29}$  clearly indicate that this resonance must be identified with the 2088-keV ( $J^\pi = \frac{1}{2}^+$ )<sup>s</sup> resonance in  $\text{Si}^{28}(p, p)\text{Si}^{28}$ .

The data for the 2084-keV resonance are shown in the left-hand portion of Fig. 12. The analysis of these data yielded the assignments  $l = 2$  and  $J^\pi = 1^+$  or  $3^+$ . The strength of the inelastic channel  $S_{pp'} = 104 \pm 22$  eV results in reduced proton widths of  $\theta_{p'}^2 = 1.24$  or  $0.53$  for  $J^\pi = 1^+$  or  $3^+$ , respectively. The value for  $J^\pi = 1^+$  exceeds the single-particle limit, making the  $1^+$  assignment unlikely. Moreover, the formation of a  $J^\pi = 1^+$  level is more likely to precede via  $s$ -wave capture; however, no  $l = 0$  contribution is observed. The conclusion is that  $J^\pi = 3^+$ .

In the region of the inelastic 2351-keV resonance, a small effect is observed in the elastic channel. However, attempts to fit this effect were unsuccessful, and it is not clear whether the effect is real. A major difficulty encountered in

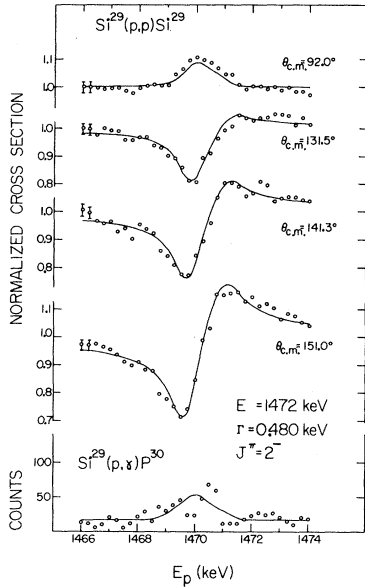


FIG. 5. The differential cross section at four angles for elastic proton scattering on  $\text{Si}^{29}$  in units of the Rutherford contribution at the  $E_p = 1472$ -keV resonance. The smooth curve is the theoretical fit for the indicated  $J^\pi$  and  $\Gamma$ . The lower curve shows the  $(p, \gamma)$  yield.

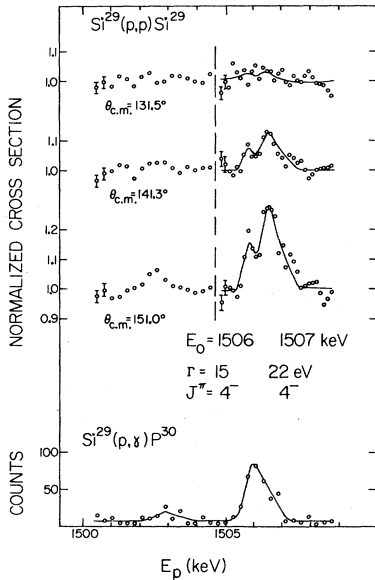


FIG. 6. The differential cross section at three angles for elastic proton scattering on  $\text{Si}^{29}$  in units of the Rutherford contribution at the  $E_p = 1502$ - and  $1506$ -keV resonances. The doublet structure of the  $1506$  resonances is apparent. The smooth curve through the  $1506$ -keV data is the theoretical fit for the indicated spins, parities, and widths. No unique  $l$  or  $J^\pi$  values were obtained for the  $1502$ -keV resonance. The lower curve shows the  $(p, \gamma)$  yield.

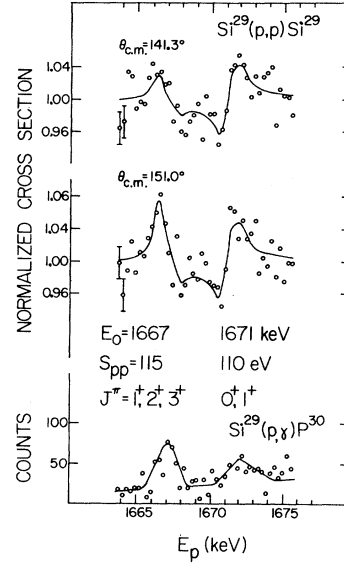


FIG. 7. The differential cross section at two angles for elastic proton scattering on  $\text{Si}^{29}$  in units of the Rutherford contribution at the  $E_p = 1667$ - and  $1672$ -keV resonances. The smooth curve is the theoretical fit for the assignments  $J^\pi(1667) = 1^+$  and  $J^\pi(1672) = 0^+$ . However, the curves for the other indicated  $J^\pi$  assignments are quite similar. Interference effects from the  $1641$ - and  $1686$ -keV resonances were taken into account in the analysis. The lower curve shows the  $(p, \gamma)$  yield.

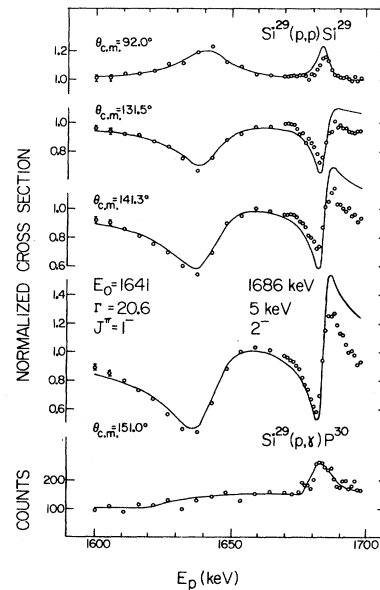


FIG. 8. The differential cross section at four angles for elastic proton scattering on  $\text{Si}^{29}$  in units of the Rutherford contribution at the  $E_p = 1641$ - and  $1686$ -keV resonances. The smooth curve is the theoretical fit for the indicated spins, parities, and widths. The poor fit to the  $1686$ -keV resonance yield is attributed to a large background from  $\text{C}^{12}(p, p)\text{C}^{12}$  (see text for details). The lower curve shows the  $(p, \gamma)$  yield.

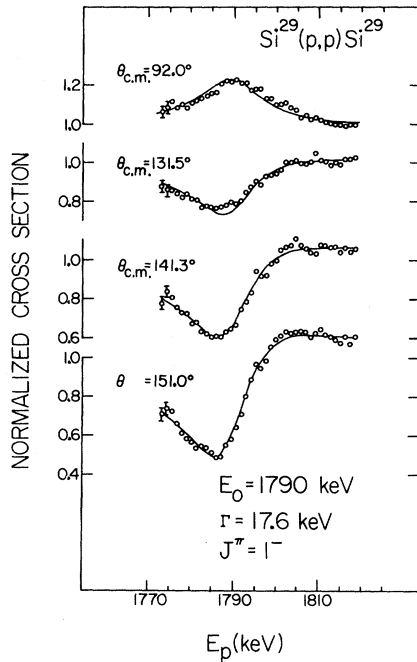


FIG. 9. The differential cross section at four angles for elastic proton scattering on  $\text{Si}^{29}$  in units of the Rutherford contribution at the  $E_p = 1790$ -keV resonance. The smooth curve is the theoretical fit for the indicated  $J^\pi$  and  $\Gamma$ .

the analysis is the strong interference effects of the 2337-, 2367-, and 2418-keV resonances. These strong interference effects are responsible

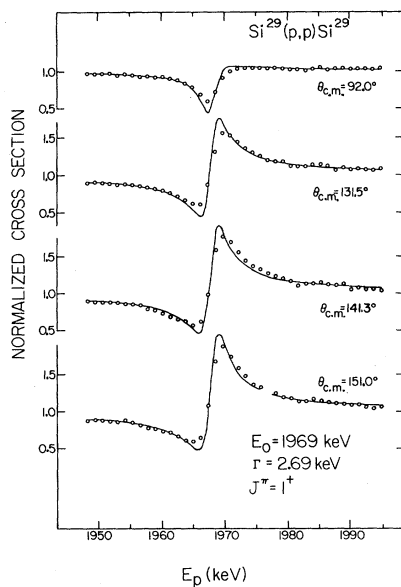


FIG. 10. The differential cross section at four angles for elastic proton scattering on  $\text{Si}^{29}$  in units of the Rutherford contribution at the  $E_p = 1969$ -keV resonance. The smooth curve is the theoretical fit for the indicated  $J^\pi$  and  $\Gamma$ .

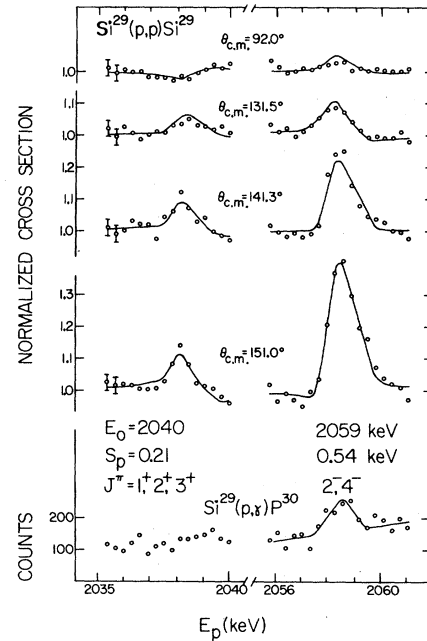


FIG. 11. The differential cross section at four angles for elastic proton scattering on  $\text{Si}^{29}$  in units of the Rutherford contribution at the  $E_p = 2040$ - and  $2059$ -keV resonances. The smooth curves are the theoretical fits for  $J^\pi(2040) = 1^+$  and  $J^\pi(2059) = 2^-$ . However, the fits for the other indicated  $J^\pi$  assignments are quite similar. The lower curve shows the  $(p, \gamma)$  yield.

for the large error quoted for the width of the 2337-keV resonance; although, the  $l$  and  $J^\pi$  assignments are unique.

The results for the 2393-keV resonance region are shown in Fig. 14. This effect was previously reported as a single resonance.<sup>3</sup> Our inelastic measurements show a broad effect centered on 2393 keV. However, attempts to fit the elastic data with a single resonance effect were unsuccessful. The data are consistent only with two interfering resonances having the parameters indicated on the figure. No attempt was made to fit the broad inelastic effect with two resonances.

## V. SUMMARY AND DISCUSSION

The final results of the elastic and inelastic proton-scattering measurements on  $\text{Si}^{29}$  are presented in Table III. The values of  $J^\pi$  enclosed in parentheses indicate possibilities not entirely excluded by the  $\chi^2$  analysis or other considerations. In these cases, the strength quantities  $S_{pp}$  and  $S_{pp'}$  are presented in lieu of the values of  $\Gamma_p$  and  $\Gamma_{p'}$ . For those resonances where the partial widths could be determined, the reduced proton widths were computed<sup>14</sup> from penetrabilities and level-shift functions based upon an assumed channel ra-



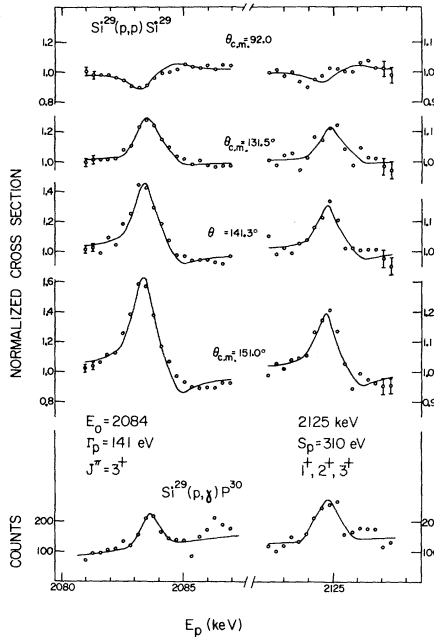


FIG. 12. The differential cross section at four angles for elastic proton scattering on  $\text{Si}^{29}$  in units of the Rutherford contribution at the  $E_p = 2084$ - and  $2125$ -keV resonances. The smooth curve through the  $2084$ -keV data is the theoretical fit for the indicated  $J^\pi$  and  $\Gamma$ . The curve through the  $2125$ -keV data is for the  $J^\pi = 1^+$  assignment. However, the other  $J^\pi$  assignments give similar fits. The lower curves show the  $(p, \gamma)$  yield.

dius  $R = r_0(A^{1/3} + 1)$  with  $r_0 = 1.2$  F. The reduced widths in single-particle units are presented in the last two columns of Table III.

The large inelastic reduced width  $\theta_p^2 = 0.53$  for the  $J^\pi = 3^+$  resonance at  $E_p = 2084$  keV is remarkable. The resonance state must be dominated by the simple configuration

$$|\text{Si}^{29}(1.27, \frac{3}{2}^+) | p(l=2) \rangle_{J^\pi=3^+}.$$

This result seems surprising in light of the rather high excitation energy,  $E_x = 7.61$  MeV, of the resonance level in  $\text{P}^{30}$ . L'vov *et al.*<sup>3</sup> have measured the angular distribution of the  $1.27$ -MeV  $\gamma$  ray resulting from the  $(p, p'\gamma)$  reaction at the resonance with the result  $W(\theta) = 1 - (0.12 \pm 0.02)P_2(\cos \theta)$ . Using the multipolarity mixing ratio  $\delta(1.27) = -0.21 \pm 0.03$  observed by McCallum,<sup>15</sup> we have analyzed<sup>16</sup> this result, for  $J^\pi(\text{Res.}) = 3^+$ , in terms of the intensity ratio  $R = d_{5/2}/d_{3/2}$  for the outgoing proton channel. The analysis yields the value  $R \leq 0.25$ , i.e., the outgoing protons are pure  $d_{3/2}$  within the errors of measurement. [For  $R = 0$  and the value  $\delta(1.27)$  given above, the coefficient of  $P_2(\cos \theta)$  in  $W(\theta)$  would be  $-0.08 \pm 0.04$ .] Straightforward considerations<sup>7</sup> of two-nucleon spectra of  $\text{P}^{30}$  suggest that a possible  $d_{3/2}^2(J, T = 3, 0)$  level

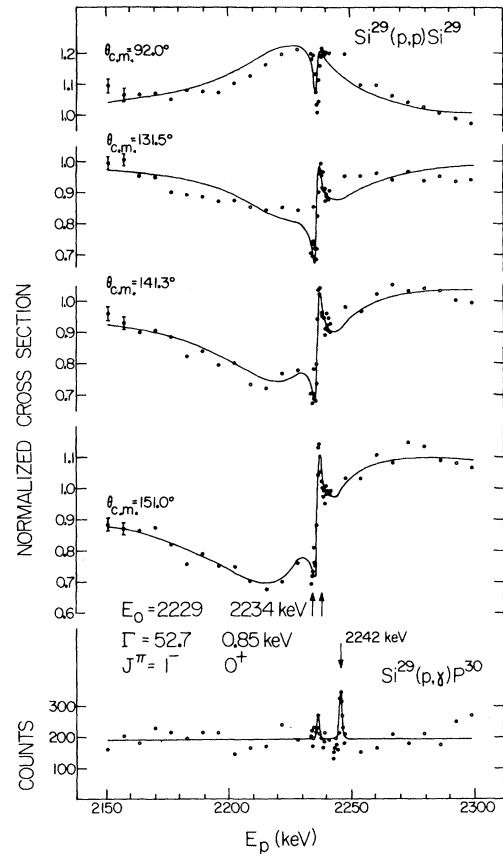


FIG. 13. The differential cross section at four angles for elastic proton scattering on  $\text{Si}^{29}$  in units of the Rutherford contribution at the  $E_p = 2229$ - and  $2234$ -keV resonances. The smooth curve is the theoretical fit for the indicated spins, parities, and widths. The lower curve shows the  $(p, \gamma)$  yield. The  $2242$ -keV resonance is observed in the  $(p, \gamma)$  channel but not in the  $(p, p)$  channel.

should lie in the region  $E_x \sim 2$ - $3$  MeV. The much higher-lying level observed here is surely not of this simple form. Its high excitation energy might be explained if it were a  $3^+$ ,  $T = 1$  level. However, the simple  $d_{3/2}^2$  configuration is not antisymmetric for  $J, T = 3, 1$ . Thus, if the resonance is a  $T = 1$  level, one may conclude that the  $1.27$ -MeV,  $\frac{3}{2}^+$  level of  $\text{Si}^{29}$  is far from a simple inert  $\text{Si}^{28}$  core plus  $d_{3/2}$  neutron configuration.

Special attention should be given to the odd-parity resonances which in many cases have elastic reduced widths on the order of 20% of the single-particle value. At least three of these resonances are believed<sup>1</sup> to be  $T = 1$  analog states - namely, the  $1506$ -keV  $T$ -mixed doublet and the  $1641$ - and  $1686$ -keV resonances. No spin and parity values or spectroscopic factors for corresponding levels in  $\text{Si}^{30}$  are known, so a direct comparison cannot be made and further identification of analog states in

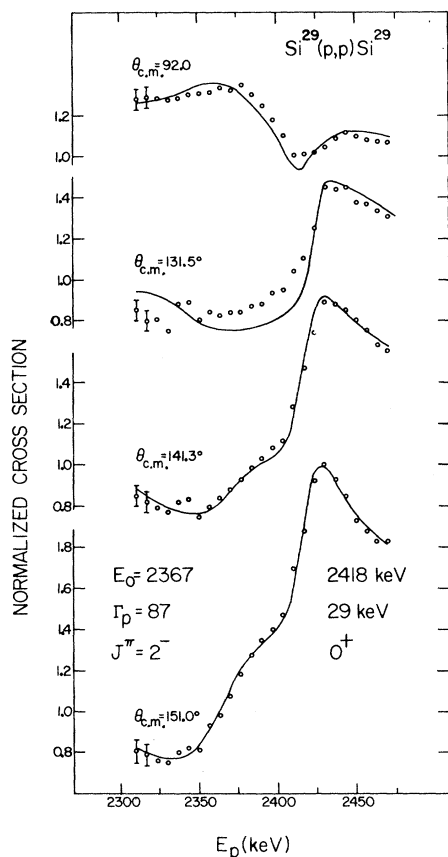


FIG. 14. The differential cross section at four angles for elastic proton scattering on  $\text{Si}^{29}$  in units of the Rutherford contribution in the 2393-keV resonance region. This effect was previously reported as a single resonance; however, the results of the present work are consistent only with two interfering resonances with the indicated energies, widths, spins, and parities.

$\text{P}^{30}$  is difficult.

Table IV lists the set of observed  $1^-$ ,  $2^-$ , and  $4^-$  resonances and their elastic reduced widths. The total  $p$ -wave reduced width,  $\theta_p^2 = 1.14$ , for the  $1^-$  resonances are quite large, but include the contribution from both  $p_{1/2}$  and  $p_{3/2}$  scattering. Conversion from channel-spin to  $jj$  coupling<sup>1</sup> yields the following relation between the values of  $\zeta$  for  $1^-$  in Table III and the amplitude ratio  $x = p_{3/2}/p_{1/2}$ :

$$\zeta = (2 - 2x + 0.5x^2)/(3 - 2x + 1.5x^2).$$

The possible values of  $x$  which satisfy this relation are shown in the third column of Table IV. The results, although not unique, show that both  $p_{1/2}$  and  $p_{3/2}$  contribute strongly in all cases. The results show, for example, that the minimum and maximum total values possible for  $\theta_p^2(p_{1/2})$  are 0.06 and 0.81, respectively. Similarly, the mini-

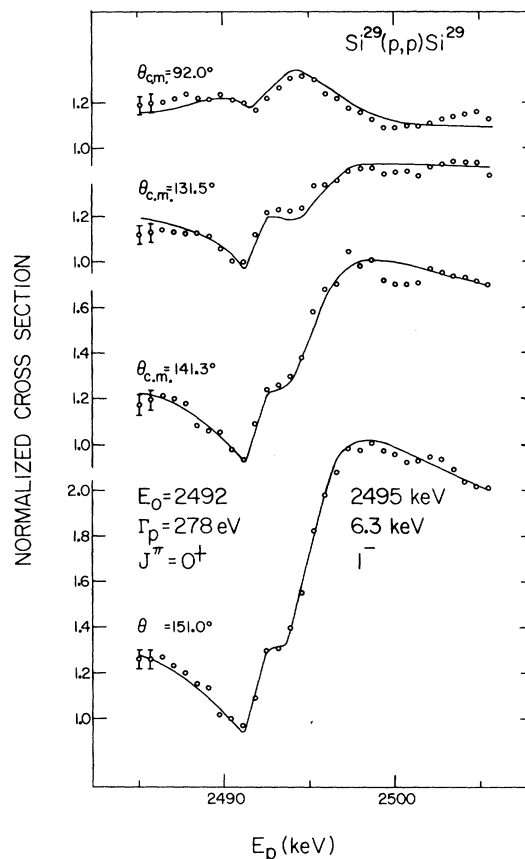


FIG. 15. The differential cross section at four angles for elastic proton scattering on  $\text{Si}^{29}$  in units of the Rutherford contribution at the  $E_p = 2492$ - and  $2495$ -keV resonances. The smooth curve is the theoretical fit for the indicated spins, parities, and widths.

imum and maximum values possible for  $\theta_p^2(p_{3/2})$  are 0.33 and 1.09.

The four observed  $2^-$  resonances (all formed by essentially pure  $p_{3/2}$  scattering) also show a large total elastic reduced width  $\theta_p^2(p_{3/2}) = 0.68$ . Similarly the  $4^-$  resonances show a total  $f_{7/2}$  reduced width of  $\theta_p^2 = 0.15$ .

Recently, shell-model calculations have been carried out by Watson and Harris<sup>7</sup> in which the odd-parity levels arising from two valence nucleons outside an inert  $\text{Si}^{28}$  core were considered. The single-particle orbits considered were  $2s_{1/2}$ ,  $1d_{3/2}$ ,  $1f_{7/2}$ ,  $2p_{3/2}$ ,  $1f_{5/2}$ , and  $2p_{1/2}$ . The two-body matrix elements were derived from the modified surface  $\delta$  interaction.<sup>17</sup> The four parameters of this interaction and the six single-particle energies were adjusted to fit 25 experimental levels in  $\text{Si}^{29}$ ,  $\text{P}^{29}$ ,  $\text{Si}^{30}$ , and  $\text{P}^{30}$  with a resulting average deviation of about 0.2 MeV between the calculated and experimental levels. The calculated two-nucleon spectrum for  $\text{P}^{30}$  has 28 odd-parity levels

TABLE III. Results of the present experiment. Numbers in parentheses are the errors in the last digit(s). In those cases where  $\Gamma_{p'} \approx 0$ , only  $\Gamma_t$  is listed. See Ref. 1 for information on  $\Gamma_\gamma$  and  $S_{p\gamma}$ .

$E_p$ (keV)	$l$	$J^\pi$	$\xi$	$\Gamma_p$ (keV)	$\Gamma_{p'}$ (eV)	$\Gamma_t$ (keV)	$S_{pp}$ (keV)	$S_{pp'}$ (eV)	$10^2\theta_p^2$	$10^2\theta_{p'}^2$
1302.2(5)	0	$1^+$	1.0			0.017(5)			0.04	
	1	$1^-$	0.67							
1326.7(5)	1	$2^-$	1.0			4.0(2)			27.5	
1372.8(5)	1	$1^-$	0.06(3) <sup>a</sup>			5.6(6)			30.3	
1472.3(5)	1	$2^-$	1.0			0.48(2)			1.73	
1501.7(5)							0.05(2)			
1505.8(3)	3	$4^-$	1.0			0.015(2)			5.21	
1506.5(3)	3	$4^-$	1.0			0.022(2)			7.64	
1641.2(5)	1	$1^-$	0.49(2) <sup>a</sup>			20.0(10)			39.6	
1667.0(5)	2	$2^+(1^+, 3^+)$	...				0.12(2)		0.3	
1671.5(5)	0	$1^+(0^+)$	...				0.11(2)		0.03	
1686(2)	1	$2^-$	1.0			5.0(10)			8.3	
1789.9(5)	1	$1^-$	0.53(4)			18.0(10)			21.3	
1968.6(5)	0	$1^+$	1.0	2.69(5)	11(2)				0.86	2.23
2039.8(5)	2	$1^+, 2^+, 3^+$	...				0.21(3)	19(4)		
2058.6(5)	3	$2^-, 4^-, (3^-)$	...				0.54(3)			
2083.8(5)	2	$3^+$	1.0	0.14(4)	15(3)				0.41	53.3
2125.2(5)	2	$1^+, 2^+, 3^+$	...				0.31(3)			
2229(1)	1	$1^-$	0.34(2)	53(3)	14(3)				21.2	1.29
2234.1(5)	0	$0^+$	0.0	0.85(4)	110(25)				0.15	2.74
2314.2(5)								240(5)		
2337(2)	0	$0^+$	0.0	15(7)	4(2)				2.54	0.05
2351(2)								7(2)		
2367(2)	1	$2^-$	1.0	87(3)	80(20)				30.4	2.19
2412(2)	2	$1^+, 2^+, 3^+$	...				0.44(5)	120(30)		
2418(2)	0	$0^+$	0.0			29(2)			4.46	
2492(2)	0	$0^+$	0.0			0.28(4)			0.04	
2495(2)	1	$1^-$	0.43(5)	6.3(4)	430(90)				1.90	6.57

<sup>a</sup>Values of  $\xi$  from Ref. 1 used in the analysis of the  $(p, p)$  data.

in the range  $E_x = 4-8$  MeV to compare with 20 known odd-parity levels. The energy regions

TABLE IV. Elastic proton reduced widths in single-particle units for  $1^-$ ,  $2^-$ , and  $4^-$  resonances observed in the present work. The quantity  $x$  gives the amplitude ratio of  $p_{3/2}/p_{1/2}$  contribution at the  $J^\pi = 1^-$  resonances.

$E_p$ (keV)	$J^\pi$ (Res.)	$l_p$	$10^2\theta_p^2$	$x$
1373	$1^-$	1	30.3	$1.41 \pm 0.15$ or $3.1 \pm 0.5$
1641	$1^-$	1	39.6	$0.46 \pm 0.05$ or $-4.8 \pm 0.9$
1790	$1^-$	1	21.3	$0.38 \pm 0.10$ or $-3.6 \pm 1.2$
2229	$1^-$	1	21.2	$0.74 \pm 0.04$ or $ x  \geq 20$
2495	$1^-$	1	1.90	$0.58 \pm 0.09$ or $ x  \geq 5$
1327	$2^-$	1	27.5	
1472	$2^-$	1	1.73	
1686	$2^-$	1	8.3	
2367	$2^-$	1	30.4	
1505.8	$4^-$	3	5.2	
1506.5	$4^-$	3	7.6	
2059	$(4)^-$	3	(2.3) <sup>a</sup>	

<sup>a</sup> $\theta_p^2$  based upon the most likely assignment of  $4^-$  for the  $E_p = 2059$ -keV resonance.

where large reduced widths for a specific  $J^\pi$  occur are well reproduced. In the region covered by the present work, total calculated values for  $\theta_p^2$  of 0.81, 0.52, and 0.50 for  $J^\pi = 1^-$ ,  $2^-$ , and  $4^-$  levels, respectively, were obtained. These compare reasonably well with the corresponding observed values  $\theta_p^2 = 1.14, 0.68, \text{ and } 0.15$ . The calculations also predict a total strength of  $\theta_p^2 = 0.12$  for  $3^-$  levels and one  $T=0, 0^-$  level with  $\theta_p^2(p_{1/2}) = 0.4$  in the region investigated.

A detailed result of the model calculation of special interest to the present work is the prediction of two close-lying  $4^-$  levels near  $E_x = 7.0$  MeV in  $P^{30}$ . Both levels lie within 0.2 MeV of the excitation energy,  $E_x = 7.05$  MeV, corresponding to the  $T$ -mixed  $4^-$  doublet observed at  $E_p = 1506$  keV. One of the calculated  $4^-$  levels has the dominant configuration  $|s_{1/2} f_{7/2}(4^-, T=1)\rangle$ , and the other has the dominant configuration  $|d_{3/2} f_{5/2}(4^-, T=0)\rangle$ . These levels, which if by chance lie very close together, would mix via the Coulomb interaction and could explain in a simple manner the split  $4^-$  analog state with components separated by only 0.7

keV. Another 4<sup>-</sup>,  $T=1$  level with major configuration  $|d_{3/2}f_{7/2}\rangle$  is predicted within 0.25 MeV of the probable 4<sup>-</sup> level observed at  $E_p = 2059$  keV.

Another result worth mentioning is the prediction of a 3<sup>-</sup>,  $T=1$  level at an excitation energy corresponding to  $E_p = 2.80$  MeV. Such a level at  $E_p = 2.79$  MeV is expected as the analog of a known, probable 3<sup>-</sup> level at  $E_x = 7.61$  MeV in Si<sup>30</sup>. Also, Bromley *et al.*<sup>18</sup> have observed a 3<sup>-</sup> level at  $E_p = 2.80$  MeV in the Si<sup>29</sup>( $p, p'\gamma$ )Si<sup>29</sup> reaction. They show that the outgoing protons from this level are in a  $p_{3/2}$  state in pleasing agreement with the predicted major resonance configuration  $|d_{3/2}p_{3/2}\rangle$ .

A further ( $p, \gamma$ ) investigation in the energy re-

gion above  $E_p = 1.8$  MeV would be helpful to remove uncertainties in some spin assignments. A detailed study of higher levels in Si<sup>30</sup>, especially in the excitation energy region  $E_x = 5-8$  MeV, could be very useful in identifying analog levels and would yield further insight into the nature of the odd-parity spectrum.

#### ACKNOWLEDGMENT

We wish to express our thanks for the assistance of W. A. Anderson and P. Kivet in the long periods of data collection.

\*Visiting Research Associate under Air Force-Ohio State University Research Foundation Contract No. F 33615-67-C-1758.

†An element of the Office of Aerospace Research, U.S. Air Force.

<sup>1</sup>G. I. Harris, A. K. Hyder, Jr., and J. Walinga, *Phys. Rev.* **187**, 1413 (1969).

<sup>2</sup>V. E. Storizhko and A. I. Popov, *Izv. Akad. Nauk. SSSR Ser. Fiz.* **28**, 1152 (1964) [transl.: *Bull. Acad. Sci. USSR Phys. Ser.* **28**, 1054 (1964)].

<sup>3</sup>A. N. L'vov, A. I. Popov, P. V. Sorokin, and V. E. Storizhko, *Izv. Akad. Nauk. SSSR Ser. Fiz.* **30**, 439 (1966) [transl.: *Bull. Acad. Sci. USSR Phys. Ser.* **30**, 447 (1966)].

<sup>4</sup>S. Bergström-Rohlin, *Arkiv Fysik* **35**, 349 (1968).

<sup>5</sup>P. A. Phelps, E. A. Milne, and H. E. Handler, *Phys. Rev.* **138**, B1088 (1965).

<sup>6</sup>P. M. Endt and C. van der Leun, *Nucl. Phys.* **A105**, 1 (1967).

<sup>7</sup>D. D. Watson and G. I. Harris, in Proceedings of the International Conference on Properties of Nuclear States, Montreal, Canada, 1969, edited by M. Harvey *et al.* (Presses de l'Université de Montréal, Montréal, Canada, 1969).

<sup>8</sup>S. D. Sharma and J. P. Davidson, *Bull. Am. Phys. Soc.*

**14**, 1205 (1969); and private communication.

<sup>9</sup>The enriched Si<sup>29</sup> was obtained from Oak Ridge National Laboratory in the form of SiO<sub>2</sub> with isotopic composition: Si<sup>28</sup>(4.36%), Si<sup>29</sup>(95.28%), Si<sup>30</sup>(0.36%).

<sup>10</sup>J. Walinga, H. A. Van Rinsvelt, and P. M. Endt, *Physica* **32**, 954 (1966).

<sup>11</sup>J. M. Blatt and L. C. Biedenharn, *Rev. Mod. Phys.* **24**, 258 (1952).

<sup>12</sup>J. Walinga, *Physica* **36**, 215 (1967).

<sup>13</sup>F. W. Prosser, Jr. and G. I. Harris (unpublished).

<sup>14</sup>The program used for these calculations is a modification of one kindly made available to us by Dr. J. P. Schiffer of Argonne National Laboratory.

<sup>15</sup>G. J. McCallum, *Phys. Rev.* **123**, 568 (1961). The sign used for  $\delta$  is opposite that given by McCallum in order to be consistent with the phase convention of Ref. 16.

<sup>16</sup>W. T. Sharp, J. M. Kennedy, B. J. Sears, and M. G. Hoyle, Atomic Energy of Canada, Ltd. Report No. CRT-556, AECL-97, 1957 (unpublished).

<sup>17</sup>P. W. M. Glaudemans, P. J. Brussaard, and B. H. Wildenthal, *Nucl. Phys.* **A102**, 593 (1967).

<sup>18</sup>D. A. Bromley, H. E. Gove, E. B. Paul, A. E. Litherland, and E. Almqvist, *Can. J. Phys.* **35**, 1042 (1957).